Nanoscale

Accepted Manuscript

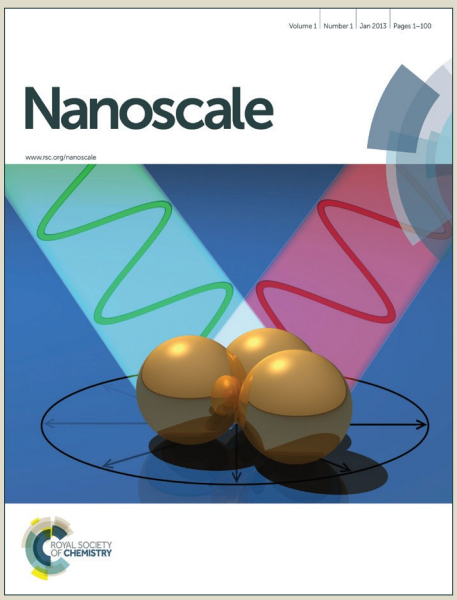

ROYAL SOCIETY OF CHEMISTRY

www.rsc.org/nanoscale

Journal Name

COMMUNICATION

Functionalized nanomaterials: are they effective to perform gene delivery to difficult-to-transfect cells with no cytotoxicity?

Received 00th January 20xx,
Accepted 00th January 20xx

DOI: 10.1039/x0xx00000x

www.rsc.org/

F. M. P. Tonelli,[a]S. M. S. N. Lacerda,[b]N. C. O. Paiva,[a]F. G. Pacheco,[c]S. R. A. ScalzoJunior,[d]F. H. P. de Macedo,[e]J. S. Cruz,[e]M. C. X. Pinto,[a]Corrêa Junior, J. D.,[f]L. O. Ladeira,[g]L. R. França,[b]S. Guatimosim,[d]and R. R. Resende[a]

Nanodiamonds (NDs), multiwall carbon nanotubes (MWCNTs) and gold nanorods (NRs) can be functionalized to promote gene delivery to hard-to-transfect cells with higher transfection efficiency than cationic lipids, and inducing less cell death rates.

Nanomaterials are important tools to be used when performing gene delivery to cells, especially mammalian cells. Among the wide array of nanomaterials available to delivery genes are:carbon – based nanomaterials such as nano graphene oxide (NGO)[1], carbon nanotubes (CNTs)[2,3], and nanodiamonds (NDs)[4], and nanomaterials not based in carbon such as gold nanorods (NRs)[5],and new nanomaterials that are continuously being proposed. However there are mammalian cells considered difficult-to-transfect cells, or hard-to-transfect cells, which are target cells when developing new reagents to transfection. Also there are a conflicting literature relating to cell toxicity about different nanomaterials[6-8].Here we report the success in using the previously mentioned nanomaterials, in a functionalized version, to transfect the following primary and lineage difficult-to-transfect cells: neonatal rat cardiomyocytes[9], rat dorsal root ganglion cells (DRG cells)[10], human neuroblastoma cell line U373[11] and the rat glial tumor cell line C6[12] (**Supplementary material**).

The multi-wall carbon nanotubes (MWCNTs) (average length of 200 nm, and average outer diameter of 25 nm) were produced using ethylene as the carbon source and cobalt and iron as catalysts by the chemical vapor deposition (CVD). After impurities removal by acid treatment they were functionalized for 15 minutes through oxidation in nitric/sulfuric acid[13-15]. The fMWCNTs were then washed, dried and submitted to FT-NIR (Fourier Transform Near-Infrared spectroscopy) to confirm the functionalization, to transmission electron microscopy (TEM) (**Figure 1**) and the energy dispersive X-ray (EDX) spectrum was obtained (**Figure S1**). The weight loss related to carboxylic function, determined by thermogravimetric analysis, was 6.36%[16].

The most prominent band in the spectra are located at: ~1770 cm^{-1}(due to stretching of the carbonyl functional group), ~1000 cm^{-1} (deformation of hydroxyl), ~1500 cm^{-1}(stretching of the carboxylate anion), ~ 1600 cm^{-1}(stretching of carbon nanotube skeleton)[17].

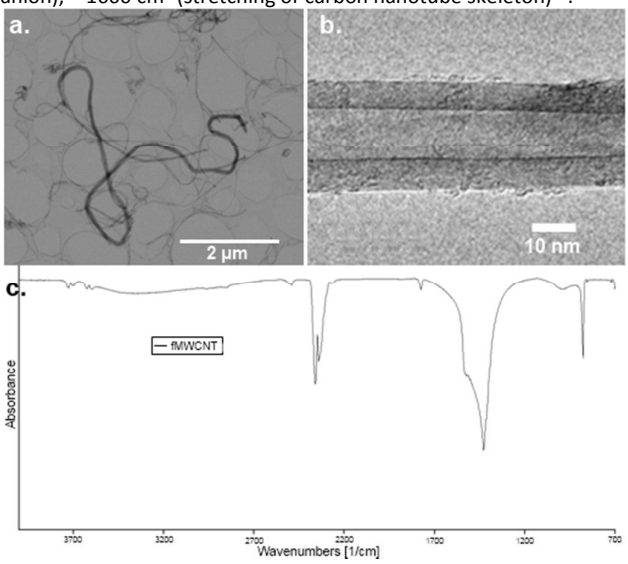

Figure 1:a. and **b.** Transmission electron microscopy (TEM) images of MWCNTs; **c.** FT-NIR spectra of fMWCNTs.

The gold nanorods were synthesized through seed-mediated growth method adapted from Nikoobakhtand El-Sayed[18]. Briefly: the seed solution was obtained by reducing, with sodiumborohydride ($NaBH_4$), a solution of cetyltrimethylammonium bromide (CTAB) and chloroauric acid ($HAuCl_4$).After 2 h at room temperature gold nanorods were obtained mixing CTAB 0.1 M, $HAuCl_4$ 10 mM, silver nitrate ($AgNO_3$) 4 mM, ascorbic acid 0.1 M, hydrochloric acid 1 M, and the seed solution. The mixture was maintained for 24 hours at 30°C then centrifuged at 5600g and

[a] Cell Signaling and Nanobiotechnology Laboratory, Department of Biochemistry and Immunology, Federal University of Minas Gerais, Belo Horizonte, Brazil.Nanocell Institute, Divinópolis, Brazil.
[b] Cell Biology Laboratory, Department of Morphology, Federal University of Minas Gerais, Belo Horizonte, Brazil.
[c] Chemistry of Nanostructures Laboratory, Nuclear Technology Development Center,Federal University of Minas Gerais, Belo Horizonte, Brazil.
[d] Cell Electrophysiology Laboratory, Department of Physiology and Pharmacology, Federal University of Minas Gerais, Belo Horizonte, Brazil.
[e] Excitable MembranesLaboratory, Department of Biochemistry and Immunology, Federal University of Minas Gerais, Belo Horizonte, Brazil.
[f] Laboratory of Biological Interaction and Animal Reproduction.Department of Morphology, Federal University of Minas Gerais, Belo Horizonte, Brazil.
Nanomaterials Laboratory, Department of Physics, Federal University of Minas Gerais, Belo Horizonte, Brazil.

redispersed in water to remove the excess of CTAB. The sample was subjected to TEM (**Figure 2**), EDX (**Figure S2**) and functionalized with phosphatidylcholine (PC)[19]. The functionalization was confirmed by spectrophotometry and FT-NIR (**Figure 2**).

The FT-NIR spectra revealed important bands that are essential for analysis of phospholipids involved in the functionalization of a nanoparticle. For example, the presence of the band at ~3400 cm^{-1} related to OH stretching not only in the PC spectra, but also in the NR-PC spectra; and the bands at ~1100, ~1200, ~2800 and ~2900 cm^{-1} in both samples, related to symmetric and antisymmetric PO_2 stretching, and symmetric and antisymmetric CH_3 stretching, respectively[20].

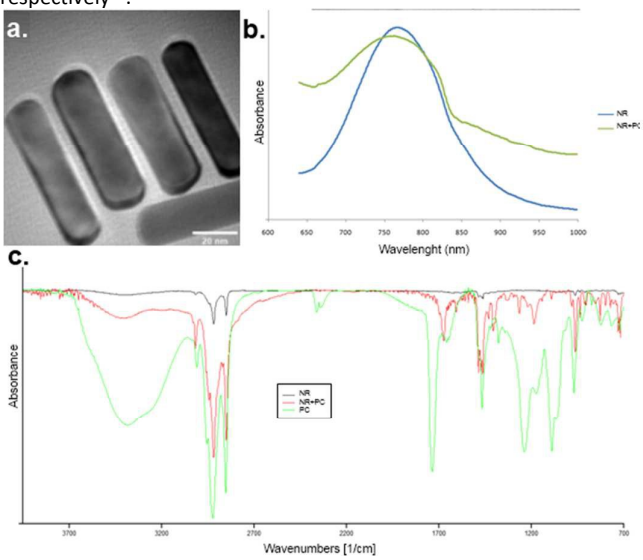

Figure 2: a. TEM image of NRs; **b.** spectrophotometric spectra of NR and functionalized NR (NR-PC); **c.** FT-NIR spectra of NR-PC, NR and PC.

The nanodiamonds were synthesized by using chitosan and acetic acid 2%. The mixture was submitted to hydrothermal treatment (180°C) inside of an autoclave for 12 hours. The solutionwas centrifuged at 8000g for 15 minutes. The NDs were submitted to TEM (**Figure 3**) and EDX (**Figure S3**), functionalized with polyethylenimine (PEI-Poly(ethyleneimine) solution ~50% in H_2O– Sigma Aldrich) in ultrasonic bath for 30 minutes and analyzed through FT-NIR (**Figure 3**).

The ND particle average size was similar to the size of nanodiamonds synthesized by Su and coworkers[21] and the FT-NIR spectra revealed important bands: a broad band from ~1700 to 1865 cm^{-1} related to carboxylic acid C=O stretch, a band in the region of 1600 cm^{-1} related to amine N–H bending (ND-PEI and PEI), and a band next to 1400 cm^{-1} related to amide CH_2 bending of of PEI. It was also possible to observe the decrease in intensity of the ND bands in the region of 3050–3650 cm^{-1} for the ND-PEI mixture: indicating that the O–H functional groups of the ND were replaced by N–H groups of PEI [22].

The nano graphene oxide was synthesized from powder graphite by using nitric acid 3.2M and sulfuric acid 0.9M. The mixture was subjected to reflux during heat in microwave oven (240W) for 3 hours. The solution was then ultra-sonicated and its pH was adjusted to 8 in ice bath. The suspension was filtered (using a 0.22µm membrane). The nanographene oxide was subjected to TEM (**Figure 4**), EDX (**Figure S4**), functionalized with polyethylenimine (PEI) in ultrasonic bath for 30 minutes and analyzed through FT-NIR (**Figure 4**).

The FT-NIR spectra of NGO-PEI presented bands from NGO and from PEI, as expected. Among the latter ones it is possible to highlight the band at ~1600 cm^{-1} (from the stretching of amide groups), and the bands at ~2900 cm^{-1} and ~2850 cm^{-1} (from methylene groups on PEI)[23].

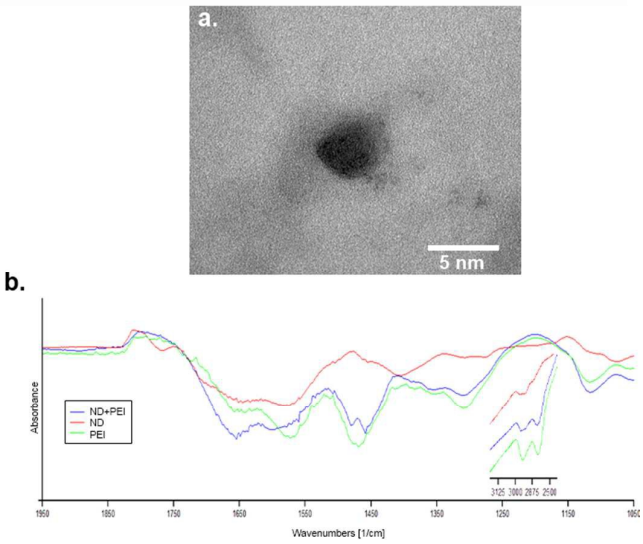

Figure 3: a.TEM image of ND; **b.**FT-NIR spectra of ND-PEI, ND and PEI. In detail, the region between 3125 and 2500 cm^{-1}.

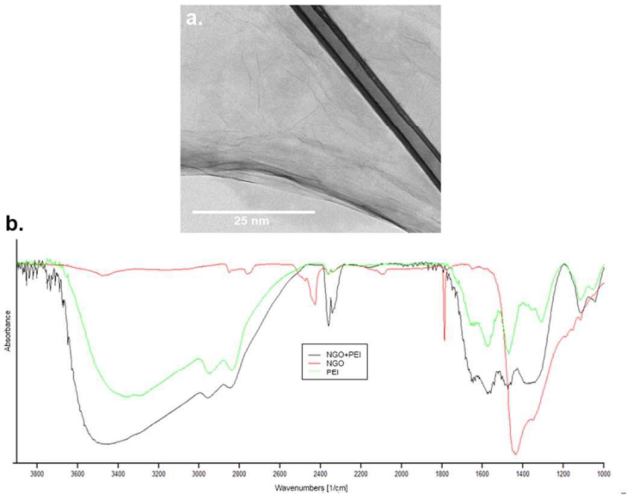

Figure 4: a.TEM image of NGO; **b.**FT-NIR spectra of functionalized ND (ND-PEI), ND and PEI.

The phosphate-based nanocomposites (NPCs) were synthesized according to two patent filing under the numbers: BR 102012032493-8 and BR 102013032731-0 available at www.inpi.gov.br. The synthesis was carried out using a mixture of salt solutions in a controlled precipitation system. The NPCs were made in liquid media using: 7mmol of $Na_4P_2O_7.10H_2O$ (Cromoline), 5 mmol of $CaCl_2.2H_2O$ (Cromoline), 5 mmol of $MgCl_2.6H_2O$ (Synth) and 3 mmol of $CrCl_3.6H_2O$ (Sigma). After synthesis, the suspension was centrifuged at 3500 rpm for 10 minutes. The precipitate was

washed three times with absolute ethanol (Merck) and dried at 60 °C for 48 hours. The sample was subjected to TEM (**Figure 5**), EDX (**Figure S5**), and analyzed through FT-NIR (**Figure 5**).

The FT-NIR spectra of NPC presented bands from P-O binding, as expected. It is possible to highlight the band at ~1100 cm^{-1} (from the stretching of P=O), the bands at ~900 cm^{-1} (stretching of P-OR esters).

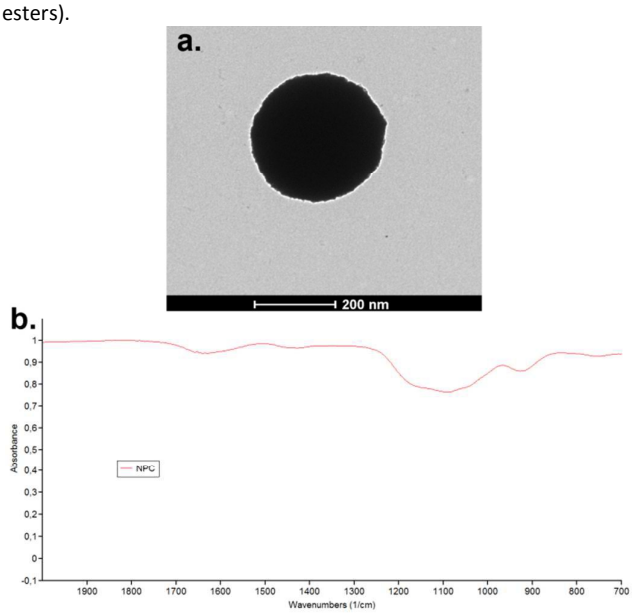

Figure 5: a.TEM image of NPC; **b.**FT-NIR spectra of NPC.

Nanomaterial concentration varied from: 0.25 mg/mL of fMWCNTs, 0.01 mg/mL of NGO, 0.1mg/mL of ND, 1.3 x 10^{13} particles/mL of NR, and 1.0 mg/mL of NPC, to values 10^{-8} inferior, through serial dilutions by a factor of 10. The concentrations 10^{-2}, 10^{-3}, 10^{-4}, 10^{-5}, 10^{-6} and 10^{-7} were conjugated to the plasmid DNA pAmCyan1-N1 (Clontech), containing the cytomegalovirus (CMV) promoter and the gene of AmCyan1 fluorescent protein, through ultrasonic bath (25 kHz, 100 W for 30 minutes), to the final concentration of 20nM of the nucleic acid. The samples were analyzed for their binding capacity (**Figure 6**) in agarose gel 0.8%, 90V using SybrSafe®.

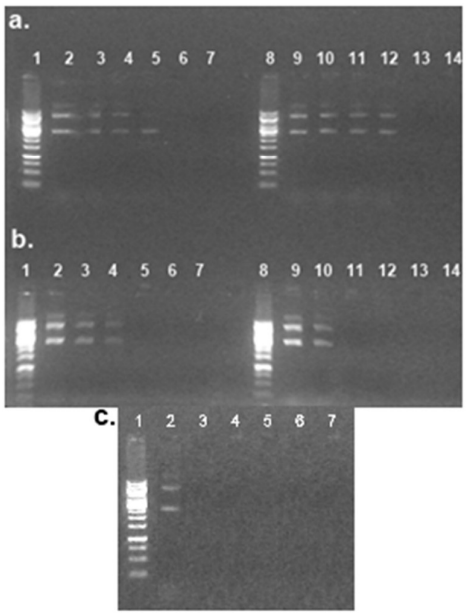

Figure 6: a. Binding capacity of NGO [Lanes 2 (10^{-7}) to 7 (10^{-2})] and ND [Lanes 9 (10^{-7}) to 14 (10^{-2})]**; b.** Binding capacity of NR [Lanes 2 (10^{-7}) to 7 (10^{-2})] and fMWCNTs [Lanes 9 (10^{-7}) to 14 (10^{-2})]. Lanes 1 and 8 – ladder 1kb; **c.** Binding capacity of NPC [Lanes 2 (10^{-7}) to 7 (10^{-2})].

Nanomaterials were all able to bind to plasmid DNA. NGO and ND from concentration 10^{-3} (10 ng/mL and 100 ng/mL, respectively) or higher; NR from 10^{-4}(1.3 x 10^{9} particles/mL) or higher; fMWCNT from 10^{-5}(2.5 ng/mL) or higher and NPC from 10^{-6}(1 ng/mL) or higher.

In order to determinate the optimal nanomaterial concentration to perform the experiments on cells, all cell types were exposed to all concentrations (from 10^{0} to 10^{-8}), and death rates assessed through Alamar Blue® assay.

Then, cells were exposed to nanomaterials in optimal concentration and complexed to plasmid DNA, and to Lipofectamine 2000® (Lipo), GeneJuice® (GJ) and X-tremeGENE™ HP DNA (XT) (according to manufacturer's recommendation) and their version complexed to DNA for 24 hours at 37°C and 5% CO_2. After this period, internalization of plasmid DNA into cells and induction of transgene expression were accessed through fluorescence microscopy (**Figures 7-10)** and RT/q-PCR (**Figures11-13**), and cell viability was assessed through Alamar Blue® assay (**Figures 14-17**). In RT-PCR experiments the oligodT primer was used to generate cDNA through the RNA extracted from cells with TRIzol® reagent, and in q-PCR the transcript generation (FWD-TTCGAGAAGATGACCGTGTG; REV-AGGTGTGGAACTGGCATCTGTA) was determined in relation to the housekeeping β-actin (FWD-ACTCTTCCAGCCTTCCTTC; REV-ATCTCCTTCTGCATCCTGTC–*Homo sapiens* and FWD-CAACTGGGACGATATGGAGAAG; REV-CTCGAAGTCTAGGGCAACATAG – *Rattus norvegicus*).

The cyan fluorescence was observed for all vehicles of gene delivery investigated for all cell types (**Figures 7-10 d, f, h, j, l, n, p, and r**), and in the absence of plasmid DNA no fluorescence was detected (**Figures 7-10 c, e, g, i, k, m, o and q**). As expected, when only the DNA (20 nM), without any delivery vehicle, was added to cell

culture (**7-10b**) there was no AmCyan1 expression, showing therefore no passive incorporation of plasmids by the cells.

When it comes to cardiomyocytes, cell death rates in transfections using fMWCNTs and NPC were significantly lower than those in which Lipofectamine was applied to perform gene delivery. Besides inducing low cytotoxic effects on cardiomyocytes, fMWCNTs as gene delivery vehicle induced higher transcription level of AmCyan1 gene than all other strategies based on nanomaterials, and also Lipofectamine; NPC presented lower cell death rates than GJ and XT also. In C6 cells fMWCNTs and NRs provided higher transcription level of AmCyan1 gene than Lipofectamine and other strategies of gene delivery based in nanomaterials; XT presented the higher transcription rate; however, NR could not only offer better efficiency than Lipofectamine, but also presented efficiency similar to the one of GJ. Cell death rates were similar for all delivery vehicles. In U373 cells commercial reagents (specially GJ) were the best way to delivery genes to cells; nanomaterials were not effective, inducing lower transcription level of AmCyan1 gene and higher cell death rates (except NPCs) than commercial reagents. In rat DRG cells NRs induced significantly lower cell death rate than Lipofectamine; the transcription level using NRs was the highest achieved among nanomaterials. NR could also present transcription level rate higher than Lipofectamine (as same as NDs and fMWCNTs), similar to the one from XT, but lower than GJ.

Characteristics such as charge and/or thickness of a cell membrane, interfere on transfection's efficiency. When it comes to U373 cells, lipid presence aids the process of delivering genes to cells (when using adenoviral particles, for example), as previously observed[24]. Thus, lipofectamine presented good delivery performance and XT offered the higher transcription level.

In conclusion, we reported here the ability of nanomaterials to transfect hard-to-transfect cells inducing low cytotoxicity. The delivery efficiency , as well as the apparent cytotoxicity, varied for each nanomaterial, and depended also on the cell type. By combining low cytotoxicity and good transfection efficiency, functionalized MWCNTs, NDs and NRs are interesting alternative strategies for gene delivery not only to common cells, but also to hard-to-transfect cells.

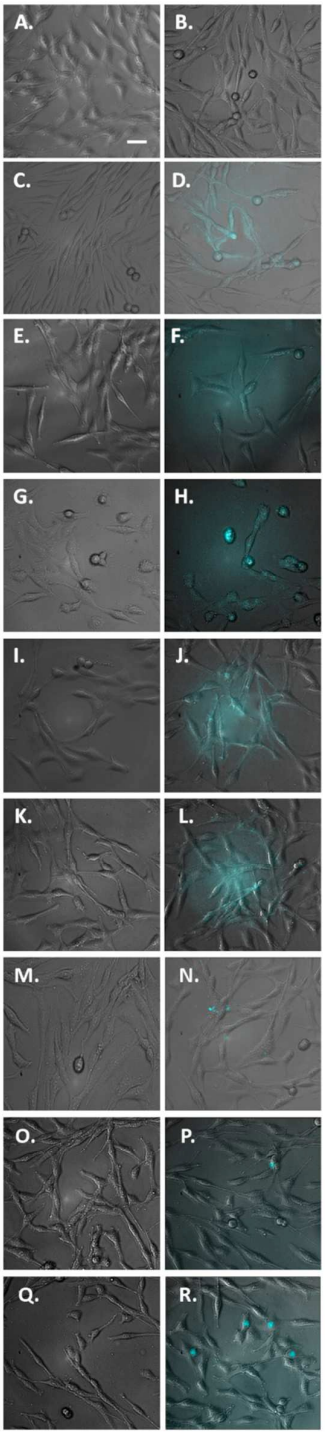

Figure7: Fluorescence microscopy images of C6 cells. (a) control; (b) DNA 20 nM and no vehicle; (c) fMWCNTs; (d) fMWCNT-DNA 20 nM; (e) Lipo; (f) Lipo-DNA 20 nM; (g) NR; (h) NR-DNA 20 nM; (i) ND; (j) ND-DNA 20 nM; (k) NGO; (l) NGO-DNA 20 Nm; (m) Nanospheres (n) Nanospheres-DNA 20 nM; (o) GJ; (p) GJ-DNA 20 nM; (q) XT; (r) XT-DNA 20 nM. Bar = 50 μm.

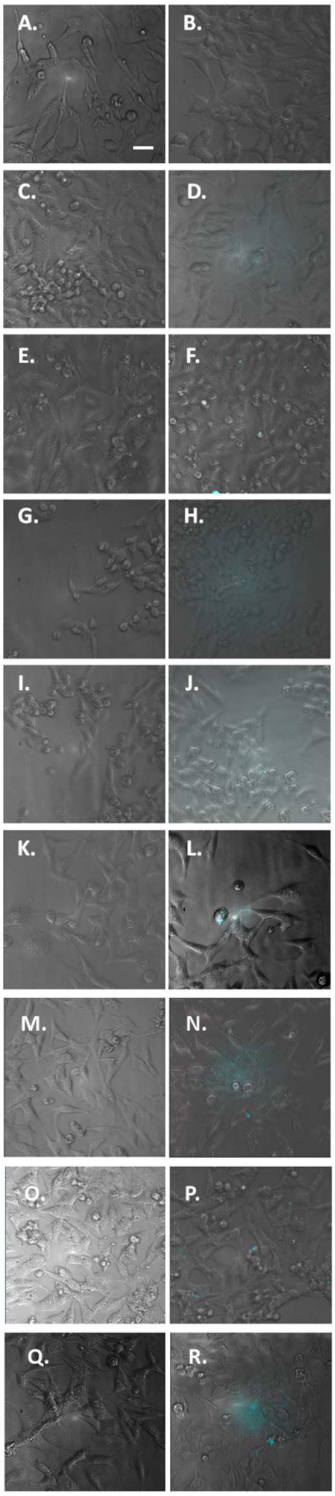

Figure8: Fluorescence microscopy images of U373 cells. (a) control; (b) DNA 20 nM and no vehicle; (c) fMWCNTs; (d) fMWCNT-DNA 20 nM; (e) Lipo; (f) Lipo-DNA 20 nM; (g) NR; (h) NR-DNA 20 nM; (i) ND; (j) ND-DNA 20 nM; (k) NGO; (l) NGO-DNA 20 Nm; (m) Nanospheres (n) Nanospheres-DNA 20 nM; (o) GJ; (p) GJ-DNA 20 nM; (q) XT; (r) XT-DNA 20 nM. Bar = 50 µm.

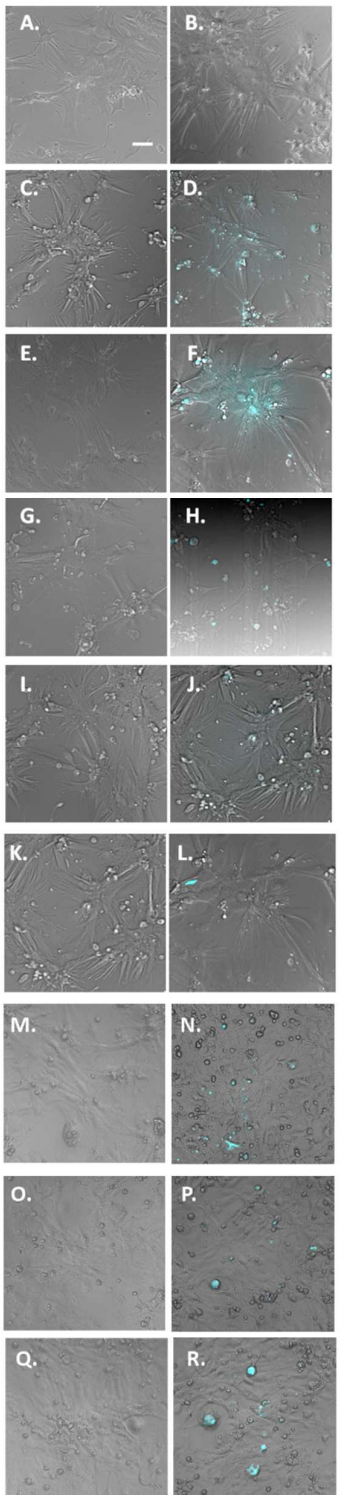

Figure9: Fluorescence microscopy images of rat cardiomyocytes. (a) control; (b) DNA 20 nM and no vehicle; (c) fMWCNTs; (d) fMWCNT-DNA 20 nM; (e) Lipo; (f) Lipo-DNA 20 nM; (g) NR; (h) NR-DNA 20 nM; (i) ND; (j) ND-DNA 20 nM; (k) NGO; (l) NGO-DNA 20 Nm; (m) Nanospheres (n) Nanospheres-DNA 20 nM; (o) GJ; (p) GJ-DNA 20 nM; (q) XT; (r) XT-DNA 20 nM. Bar = 50 µm.

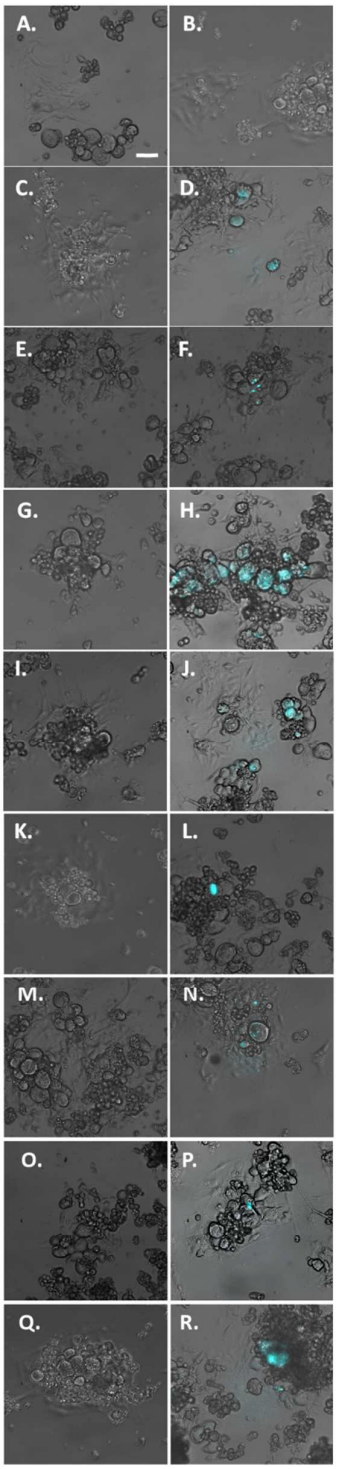

Figure 10: Fluorescence microscopy images of rat dorsal root ganglion cells. (a) control; (b) DNA 20 nM and no vehicle; (c) fMWCNTs; (d) fMWCNT-DNA 20 nM; (e) Lipo; (f) Lipo-DNA 20 nM; (g) NR; (h) NR-DNA 20 nM; (i) ND; (j) ND-DNA 20 nM; (k) NGO; (l) NGO-DNA 20 nM; (m) Nanospheres (n) Nanospheres-DNA 20 nM; (o) GJ; (p) GJ-DNA 20 nM; (q) XT; (r) XT-DNA 20 nM. Bar = 50 µm.

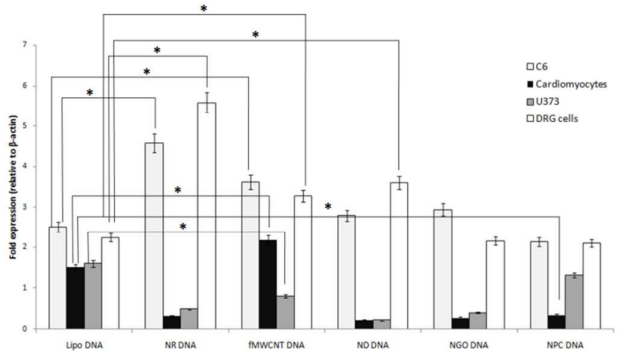

Figure 11: Dosage of transgene expression by qPCR. The values correspond to expression of AmCyan1 mRNA in relation to β-actin's in cells using different nanomaterials to promote transfection and the commercial reagent Lipofectamine 2000 (asterisk, $p < 0.05$, *t* test).

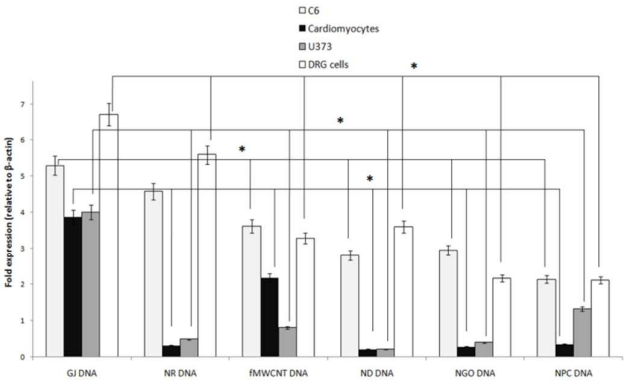

Figure 12: Dosage of transgene expression by qPCR. The values correspond to expression of AmCyan1 mRNA in relation to β-actin's in cells using different nanomaterials to promote transfection and the commercial reagent GeneJuice (asterisk, $p < 0.05$, *t* test).

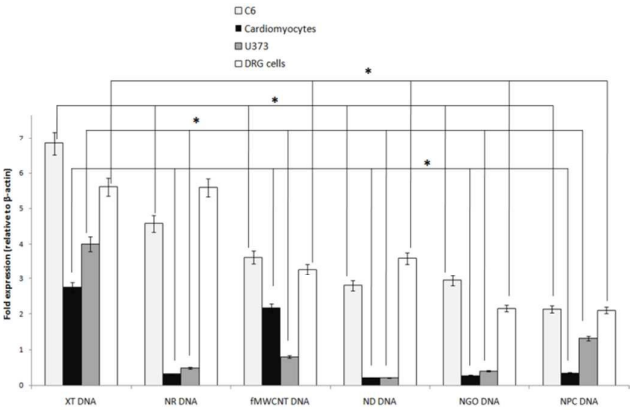

Figure 13: Dosage of transgene expression by qPCR. The values correspond to expression of AmCyan1 mRNA in relation to β-actinin cells using different nanomaterials to promote transfection and the commercial reagent X-treme (asterisk, $p < 0.05$, *t* test).

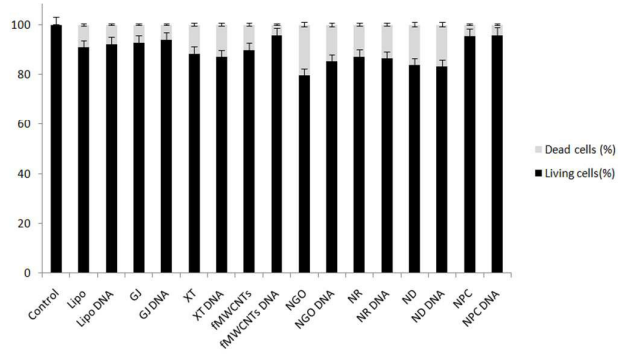

Figure 14: Percentage of dead and living C6 cells obtained through Alamar Blue® assay for the different methods of gene delivery tested.

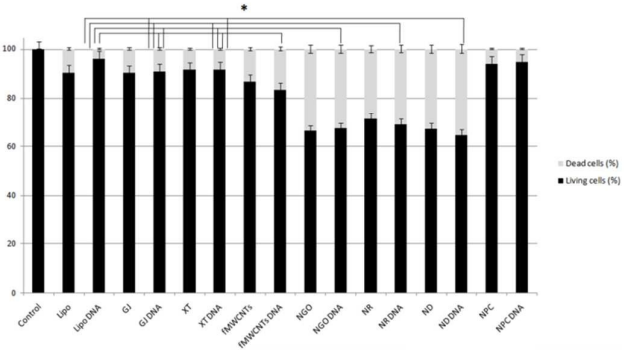

Figure 15: Percentage of dead and living U373 cells obtained through Alamar Blue® assay for the different methods of gene delivery tested (asterisk, $p < 0.05$, *t* test).

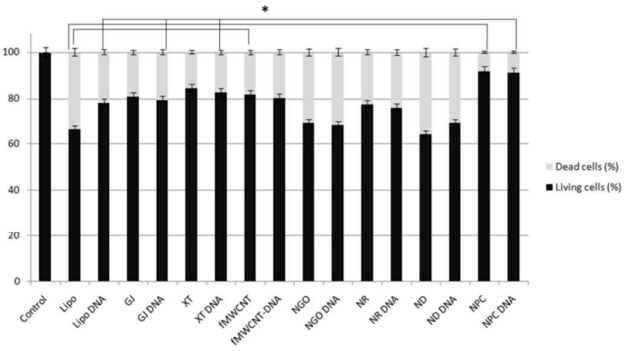

Figure 16: Percentage of dead and living cardiomyocytes obtained through Alamar Blue® assay for the different methods of gene delivery tested (asterisk, $p < 0.05$, t test).

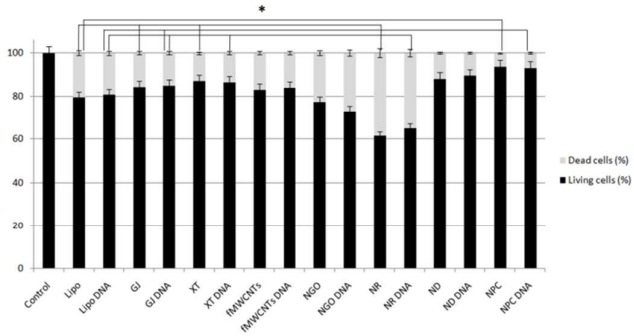

Figure 17: Dead and living rat dorsal root ganglion cells percentage obtained through Alamar Blue® assay for the different methods of gene delivery tested (asterisk, $p < 0.05$, t test).

Notes and references

1. K. Li, L. Feng, J. Shen, Q. Zhang, Z. Liu, S. T. Lee, and J. Liu, *ACS Appl Mater Interfaces*, 2014**, 6**, 5900-5907.

2. M. Karimi, N. Solati, A. Ghasemi, M. A. Estiar, M. Hashemkhani, P. Kiani, E. Mohamed, A. Saeidi, M. Taheri, P. Avci, A. R. Aref, M. Amiri, F. Baniasadi, and M. R. Hamblin, *Expert Opinion on Drug Delivery*, 2015**, 2015**, 1-17.

3. C. Geyik, S. Evran, S. Timur, and A. Telefoncu, *Biotechnology Progress*, 2014**, 30**, 224-232.

4. L. Zhao, Y. Nakae, H. Qin, T. Ito, T. Kimura, H. Kojima, L. Chan, and N. Komatsu, *Beilstein J.Org.Chem.*, 2014**, 10**, 707–713.

5. J. Ramos and K. Rege, *Biotechnol.Bioeng.*, 2012**, 109**, 1336-1346.

6. K. L. Aillon, Y. Xie, N. El-Gendy, C. J. Berkland, and M. L. Forrest, *Adv.Drug Deliv.Rev.*, 2009**, 61**, 457-466.

7. F. M. Tonelli, A. K. Santos, K. N. Gomes, E. Lorençon, S. Guatimosim, L. O. Ladeira, and R. R. Resende, *Int. J. Nanomedicine,* 2012, **7**, 4511-4529.

8. F. M. Tonelli, V. A. Goulart, K. N. Gomes, M. S. Ladeira, A. K. Santos, E. Lorençon, L. O. Ladeira, and R. R. Resende, *Nanomedicine*, 2015, **10**, 2423-2450.

9. S. Bauer, S. K. Maier, L. Neyses, and A. H. Maass, *DNA Cell Biol.*, 2005**, 24**, 381-387.

10. M. S. Ladeira, V. A. Andrade, E. R. M. Gomes, C. J. Aguiar, E. R. Moraes, J. S. Soares, E. E. Silva, R. G. Lacerda, L. O. Ladeira, A. Jorio, P. Lima, M. F. Leite, R. R. Resende, and S. Guatimosim, *Nanotechnology*, 2010**, 21**, 101-113.

11. E. A. Murphy, D. N. Streblow, J. A. Nelson, and M. F. Stinski, *J.Virol.*, 2000**, 74**, 7108-7118.

12. C. D. Wilson, B. Parameswaran, and G. R. Molloy, *J.Neurosci.Res.*, 1993**, 35**, 92-102.

13. N. G. Sahoo, H. Bao, Y. Pan, M. Pal, M. Kakran, H. K. Cheng, L. Li, and L. P. Tan, *Chem.Commun.(Camb.)*, 2011**, 47**, 5235-5237.

14. E. Lorençon, A. S. Ferlauto, S. de Oliveira, D. R. Miquita, R. R. Resende, R. G. Lacerda, and L. O. Ladeira, *ACS Appl.Mater.Interfaces*, 2009**, 1**, 2104-2106.

15. E. Lorençon, R. G. Lacerda, L. O. Ladeira, R. R. Resende, A. S. Ferlauto, U. Schuchardt, and R. M. Lago, *Journal of Thermal Analysis and Calorimetry*, 2011**, 105**, 953-959.

16. F. M. P. Tonelli, S. M. S. N. Lacerda, M. A. Silva, E. S. Avila, L. O. Ladeira, L. R. Franτa, and R. R. Resende, 2014.

17. F. A. Abuilaiwi, T. Laoui, M. Al-Harthi, and M. A. Atieh, *The Arabian Journal for Science and Engineering*, 2010**, 35**, 37-48.

18. B. Nikoobakht and M. A. El-Sayed, *Chem.Mater.*, 2003**, 15**, 1957-1962.

19. H. Takahashi, Y. Niidome, and S. Yamada, *Chem.Commun.*, 20052247-2249.

20. H. Guenzler and H. Boeck, in *IR Spectroscopy: an Introduction*, Weinheim,Germany, 2nd ed., 1983, pp. 403.

21. Z. Su, W. Zhou, and Y. Zhang, *Chem.Commun.*, 2011**, 47**, 4700-4702.

22. S. Singh, V. Thomas, D. Martyshkin, V. Kozlovskaya, E. Kharlampieva, and S. A. Catledge, *Nanotechnology*, 2014**, 25**, 1-10.

23. T. Ren, L. Li, X. Cai, H. Dong, S. Liu, and Y. Li, *Polym.Chem.*, 2012**, 3**, 2561-2569.

24. E. A. Murphy, D. N. Streblow, J. A. Nelson, and M. F. Stinski, *J. Virol.*, 2000, **74**, 7108-7118.

Nanomaterials were widely used as delivery agent for a large range of small molecules as, drugs, DNA, microRNA and others. However, an increasing data present divergent information about their toxicity. In this context, we evaluate both the toxicity and efficiency of carbon and non-carbon based nanomaterials comparing with commercial reagents through different hard-to transfect cells.

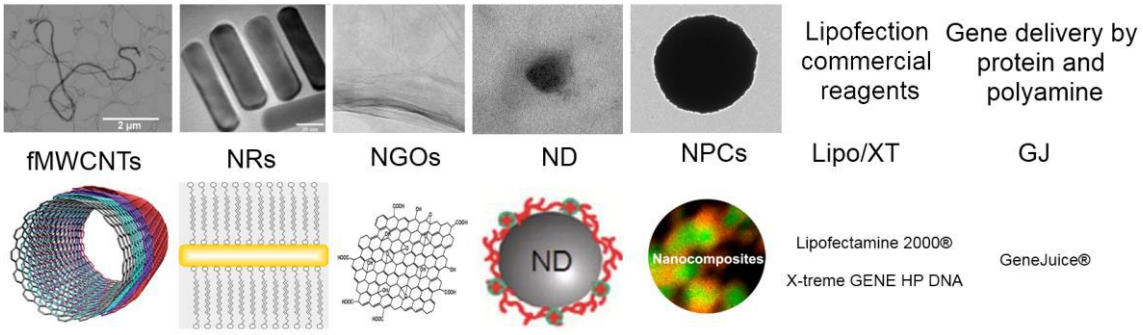

All of them were conjugated to the plasmid DNA

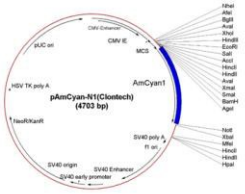

to delivery to hard-to-transfect cells

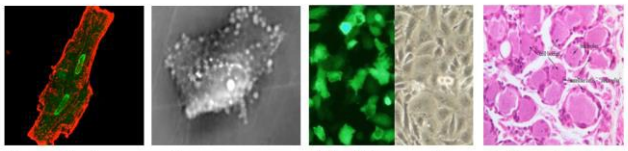

Neonatal rat cardiomyocytes | Human neuroblastoma cell line U373 | Rat glial tumor cell line C6 | Rat dorsal root ganglion cells